Microelectronic Engineering 209 (2019) 66–74

Contents lists available at ScienceDirect

Microelectronic Engineering

journal homepage: www.elsevier.com/locate/mee

Review article

Micro- and nanofabrication NMR technologies for point-of-care medical applications – A review

Antoine Dupré[a,1], Ka-Meng Lei[b,c,1], Pui-In Mak[b,d], Rui P. Martins[b,d,e], Weng Kung Peng[a,*]

[a] Precision Medicine - Engineering, Department of Nanoelectronics Engineering, International Iberian Nanotechnology Laboratory, Braga 4715-330, Portugal
[b] State Key Laboratory of Analog and Mixed-Signal VLSI, University of Macau, Macao SAR, China
[c] School of Engineering and Applied Sciences, Harvard University, Cambridge, MA 02138, USA
[d] Instituto Superior Técnico, Universidade de Lisboa, 1049-001 Lisbon, Portugal
[e] Department of Electrical and Computer Engineering, Faculty of Science and Technology, University of Macau, Macao SAR, China

ARTICLE INFO

Keywords:
Micro- and nanofabrication in NMR
Integrated system
Point-of-care medical applications

ABSTRACT

In recent years, significant advances in NMR system miniaturisation (e.g., electronic console, radio-frequency probe, microfluidic-based chip) utilising small footprint permanent magnets (< 2 Tesla) have been widely applied for point-of-care medical diagnostic. These include immuno-magnetic labelling-based profiling of tumour cells and biomolecules (DNA and proteins) and the label-free detection of various pathological states such as oxygenation/oxidation level of the blood, malaria screening, and rapid phenotyping of diabetes mellitus. In this contribution we discuss the impact of micro- and nanofabrication technologies and system integration on the miniaturisation of NMR technologies, and the recent advances in NMR-based point-of-care medical diagnosis.

1. Introduction

Nuclear Magnetic Resonance (NMR) is a robust analytical instrumentation to probe the molecular information of the materials. The strong requirement of homogeneous magnetic fields to perform highly resolved spectroscopy experiments led to bulky and expensive state-of-the-art NMR spectroscopy systems based on superconducting magnet technology. Micro-NMR (μNMR) systems, which utilise portable permanent magnets and integrated electronic chips, have emerged to provide a practical solution featuring low cost, enhanced portability, and/or minimal sample consumption. Technological advances in high-density high-performance electronics bring the μNMR systems into reality. Low-field μNMR systems are highly attractive in many disciplines such as geological prospection, food science and medical point-of-care (PoC) applications [1–3].

Transducing mechanisms based on electrical [4], optical [5] or magnetic principle [6–8] are widely considered to investigate *in vitro* biological samples for rapid and efficient PoC diagnostics. In this regard, the salient features are the integrability, selectivity, and ease of operation (labelling, operation and hardware preparation) [9]. For instance, electrical impedance based techniques, featuring an excellent CMOS integration capability have been reported [10,11]. In electrical-based biomolecule detection, however, the probes to capture the specific targets need to be immobilised on the electrode (transducer), adding burdens to the manufacturing process, corresponding cost and time of the device fabrication. The NMR-based detection, however, is attractive sponding cost and time of the device fabrication. The NMR-based detection, however, is attractive as the transducer for the nuclear spin is practically a radio-frequency coil, which is available for large scale production using standard semiconductor process. Furthermore, it does not require extensive sample preparation steps, which lowers the barrier to experiment and reduces detection time greatly. The unique ability to probe molecular information with NMR further extends the range of application for μNMR systems (e.g., molecular profiling, label-free applications, etc.).

A number of books and review articles addressing the recent advances of compact NMR systems highlight the increasing interest of this community in state-of-the-art of μNMR systems and their down-stream applications [12–15]. In this review article, however, we focus on the impact of micro- and nano-fabrication technologies and system integration on μNMR as point-of-care medical diagnostic system. This article is organised as follows. Section 2 provides a brief introduction on the theory of NMR properties. Section 3 expounds the latest progresses in NMR system miniaturisation (e.g., electronic console, radio-frequency probe and microfluidic-based chips). Section 4 reviews recent μNMR-based PoC medical applications and in Section 5 we highlight

* Corresponding author.
E-mail address: weng.kung@inl.int (W.K. Peng).
[1] Equal contribution.

https://doi.org/10.1016/j.mee.2019.02.005
Received 11 October 2018; Received in revised form 14 December 2018; Accepted 14 February 2019
Available online 20 February 2019
0167-9317/

the future outlook and concluding remark.

2. Fundamental of NMR properties

2.1. NMR spectroscopy and relaxometry

The basis of NMR properties will be elaborated here. We suggest the following excellent reference for detailed theory of spin dynamics to the readers [16]. Nuclei with an odd number of protons and/or neutrons (e.g., ^{1}H, ^{13}C, ^{31}P, etc.) possess a non-zero spin. One of the most studied nuclei is hydrogen (^{1}H) as it is the most abundant in biological samples. In this contribution, we will focus on the ^{1}H related applications in the time-domain relaxometry reports.

The nuclear spin behaves like a small magnetic bar at microscopic level. When an external static magnetic field, $\overrightarrow{B_0}$ is applied (in the z-component), it creates a net magnetisation, $\overrightarrow{M}$ measurable using standard radio-frequency engineering. Without the external magnetic field, the nuclear spins are randomly aligned with zero net magnetisation on the macroscopic level. When a nucleus with spin = 1/2 is placed inside a strong external magnetic field, the spin interacts with the field, creating an energy level of $E_m = -\vec{\mu} \cdot \overrightarrow{B_0}$, where $\vec{\mu}$ is the magnetic moment of the nucleus. The magnetic field exerts a torque on the nucleus spin causing the spin to precess about the direction of z-component. The frequency of the precession is known as Larmor frequency f_L, expressed as $\gamma/2\pi \times B_0$, with γ the gyromagnetic ratio of the nuclei of interest.

A strong radiofrequency pulse orthogonal to the z-axis, $\overrightarrow{B_1}$ is applied at f_L to tip the spins towards the x-y plane. The tipping angle is proportional to the magnitude and duration of the pulse. A tip angle of 90° (i.e., in the x-y plane) maximises the resultant of NMR signal in the transverse plane, upon which the spins will return to z-component defined by the thermal equilibrium. The radio-frequency coil detects the transverse magnetization of the spins known as free-induction decay (FID) signal. The magnitude of the voltage induced is proportional to the rate of change of the magnetic flux.

In spectroscopy experiments, the structure of the molecules affects the precession frequencies of the nuclei [17]. For ^{1}H, the shifts in frequency are typically in the order of parts per million (ppm). Therefore, a highly homogenous $\overrightarrow{B_0}$ field is a strong prerequisite for high spectral resolution works. Such systems require highly homogeneous samples and susceptibility matching within the samples, coil, and container, which became one of the major obstacles towards PoC applications.

On the other hand, vital molecular information can be captured by exploiting the relaxation properties, in both the longitudinal (z-axis) and transverse (xy-plane) plane [18]. The longitudinal relaxation time constant T_1 is recorded using the inversion-recovery sequences, while the transverse relaxation time constant denoted as T_2, can be obtained using Carr-Purcell-Meiboom-Gill (CPMG) pulse sequences [16]. The relaxation rates R_1 and R_2, is given by the inverse of the T_1 and T_2, $R_1 = 1/T_1$ and $R_2 = 1/T_2$, respectively. Unlike the frequency domain, relaxometry experiments have much lower requirements for $\overrightarrow{B_0}$ field homogeneity as typically they do not require high spectral resolution.

3. The NMR architecture and engineering

3.1. Electronic chip – integrated circuit

Modern nanometre-scale Integrated Circuit (IC) technologies have profound impact in the development of μNMR systems in terms of portability of the relevant electronics. The resulting freedom to choose the impedance that can be used for optimising the transmission efficiency and/or detection sensitivity is a great benefit for the quality of the NMR measurements [8]. The transmission efficiency can be optimised with a series resonant LC matching circuit that minimises the effective impedance, and the receiver noise figure can be optimised with a parallel LC matching circuit providing a noise-free pre-amplification of both the induced voltage and the coil thermal noise. Additionally, the capability to customise and integrate different modules (e.g. temperature sensor, B_0-field stabilisation [19]) on a monolithic IC finds enormously fruitful functions in the μNMR systems.

The standard architecture of the transceiver electronics includes the microcoil and matching circuit (called micro-resonator), the transmitter (TX) and receiver (RX) chains, and a duplexer providing isolation during pulse excitation. The TX chain primarily includes a pulse programmer (PPG) to generate the excitation pulse sequence according to the NMR experiment and a power amplifier (PA) connected to the duplexer to drive the micro-resonator. The RX chain includes a Low-Noise Amplifier (LNA), a mixer, an optional Low-Pass Filter (LPF), an Intermediate Frequency (IF) amplifier and an Analog-to-Digital Converter (ADC). The forefront LNA amplifies the NMR signal coupled from the micro-resonator. With the noise figure of a RX mostly determined by prior stages (assuming those stages have high gains), their noises should be minimised to improve the noise performance. Then, the signals are fed to the mixer, which down-converts the signal to IF. As the NMR signal is at f_L and usually only occupies a small bandwidth, down-converting to IF can limit the in-band noise of the signal and facilitate the subsequent signal processing. Then, the IF amplifier and LPF further amplify the signal and remove the out of band noise as well as the undesirable high-frequency by-product from the mixer. Finally, an ADC digitises the signal to the digital domain for data storage and processing. On the other hand, the frequency synthesizer can be integrated, as reported in [20], to generate the oscillation signal for both TX and RX. Depending on the criteria and the design specifications, the IC can have different parts integrated.

3.1.1. Discrete IC

The advancement of commercial IC modules aids the miniaturisation of the NMR front-end electronics. They provide specific functions (frequency synthesis, signal amplification, filtering, etc.) and can be exchanged and fine-tuned easily for modular application at low-cost. Although they provide less design freedom when compared with the customised IC, the time required to design the electronics with discrete modules can be minimised as the customised IC consumes significant lead time from the semiconductor foundry. For example, the group at Massachusetts General Hospital proposed the use of a commercial IC to realise the μNMR electronics. They used the magnetic labels (Magnetic nanoparticles) to enhance the relaxation rate of the NMR signal in medical diagnosis applications and proposed the “Diagnostic Magnetic Resonance” (DMR) system (Fig. 1) [6]. They also integrated the system with a microfluidic channel to achieve mixing of the sample and the magnetic labels. Later, an updated version of the μNMR system from the same group emerged [21]. The system implemented with drift tracking and compensation, as well as mobile-device interface features, facilitating the overall control and culminates in a user-friendly system with clinical potential.

3.1.2. FPGA-based chip

Field-Programmable Gate Arrays (FPGAs) are general-purpose and reconfigurable integrated circuits. Arrays of programmable logic blocks can be interconnected according to the specifications of the program designer. FPGA has been widely used in the research and early development of digital and mixed-signal integrated circuit design. Several NMR spectrometers implemented by FPGA development platform have been reported. Takeda [22] developed and published the open-source code for the configuration of a FPGA-based spectrometer. The chip used is one of the *“Cyclone II”* device family by Altera (EP2C70F672C8). The digital modules include three pulse programmers, the digital parts of a DDS, a digital quadrature demodulator, dual digital low-pass filters, and a PC interface. Analog modules of the TX (DAC, LPF) and RX chains (LNA, LPF, Mixer) were not integrated into the FPGA platform. Some spectrometrapplications were demonstrated for high-field NMR

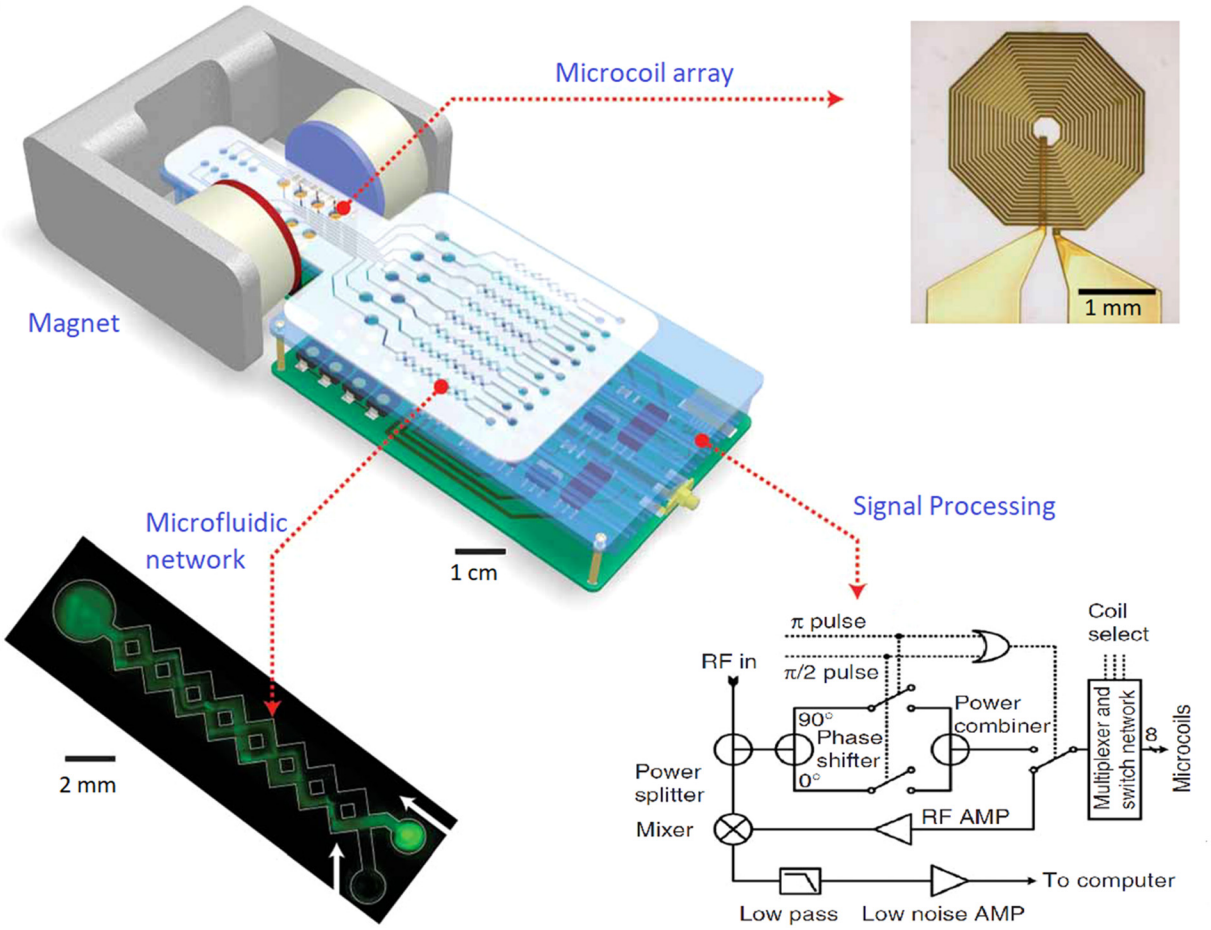

Fig. 1. Schematic diagram of the portable μNMR system consisting of a CMOS chip, permanent magnet, and microfluidic network. This figure is adapted from [6] and reproduced with permission from Springer Nature.

applications. Peng et al. integrated the FPGA chip (Cyclone III) with compact lumped-circuit duplexer and single-board 1 W power amplifier [7]. Relaxometry biomedical applications were demonstrated with this μNMR system using a compact disk magnet and electronic boards (19cm × 16cm) further improved the system portability on a single mother board (16cm × 5cm, 250 g) [7]. An FPGA implementation of a Quadrature Amplitude Modulator based on Coordinate Rotation Digital Computer (CORDIC) architecture were proposed as a replacement of physical on-board multipliers [23].

3.1.3. Integrated CMOS IC

Monolithic Complementary Metal-Oxide Semiconductor (CMOS) technology provides an optimal platform to implement digital and analogue modules of the NMR electronics with an unequalled design freedom and at a modest production cost. By utilising the miniaturised IC and placing the microcoil in close proximity (when compared with the wavelength of the signal at f_L), the need for 50-Ω impedance matching between coil and IC can be averted. This significantly simplifies the electronics and improves the overall signal-to-noise ratio [24]. Sensors for NMR microscopy (imaging at the resolution of micrometre-range) usually only integrate RX [25,26] with an external excitation coil, while systems for NMR spectroscopy and relaxometry usually co-integrate RX and TX [20,27].

Important achievements in the subfield of CMOS-integration in μNMR systems, particularly for the transceiver have been accomplished in recent decades. The group at Harvard University presented a partial 0.18 μm-CMOS implementation of the transceiver [28], with the power amplifier, micro-resonator, clock and IF signal processing not implemented into CMOS. Significant improvements in the μNMR system were reported in [29], with integration of the power amplifier. Furthermore, a variant of the system with a planar coil directly interfacing the CMOS chip is the first reported single-chip NMR system. Lei and his team presented a handheld CMOS NMR platform [19]. The group demonstrated the detection and analysis of the chemical/biological assay such as DNA/protein identification and protein aggregation with high level of integration in a monolithic CMOS chip, including a crystal oscillator to generate the reference signal.

In NMR microscopy, compact arrays of micro-sensors based on fully-integrated CMOS chips were developed to enable finer spatial resolution [25]. [20] proposed a single-chip NMR transceiver for multi-nuclear spectroscopy. Compared with other works, they integrated a frequency synthesizer to generate oscillation signal at different frequencies. As such, the IC can support probing different nuclei, i.e. varied f_L, without an external frequency synthesizer. Still, it entailed a superconducting magnet to generate the necessary high and homogeneous $\overrightarrow{B_0}$-field for spectroscopy. [30] presented the first low-field μNMR spectroscopy system with a compact magnet (weighting 7.3 kg). The work complements the miniaturisation of permanent magnets with high field homogeneity based on electrical shimming. The 2 × 2 mm^2 chip developed in the study includes transceiver modules except for the local oscillator, ADC and the off-chip solenoid microcoil. The pulse sequence synthesizer generates the pulse with various phases for different kinds of 1D (free induction decay) and 2D (correlation spectroscopy, heteronuclear multiple-quantum coherence spectroscopy, etc.) NMR experiments. Spectra of light molecules (water, ethanol, aspirin, etc.) were demonstrated by the research group [30]. Table 1

Table 1
Level of integration of the recent CMOS based μNMR technologies.

Reference	Liu [28]	Anders [25]	Sun [29]	Kim [20]	Ha [30]	Grisi [27]	Anders [26]	Lei [19]
CMOS process	180 nm	350 nm	180 nm	130 nm	180 nm	130 nm	130 nm	180 nm
B_0-field [T]	0.5	7	0.49	5	0.51	7	7	0.46
Frequency [MHz]	21.3	300	20.9	5–300	21.8	1–1000	300	19.6
Input ref. noise [nV/√Hz]	2.5	0.7	1.26	3.5	0.9	1.1	1.3	–
Chip area [mm^2]	3.8	1.02	1.96	2	4	1	1	7.6
Integration	TX/RX	RX	TX/RX	TX/RX	TX/RX	TX/RX	RX	TX/RX
Pulse sequencer	Yes	–	Yes	Yes	Yes	No	–	Yes
Power Amplifier (PA)	No	–	Yes	Yes	Yes	Yes	–	Yes
Low-Noise Amplifier (LNA)	Yes	Yes	Yes	Yes	Yes	Yes	Yes	Yes
Mixers	Yes	Yes	Yes	Yes	Yes	Yes	Yes	Yes
Low-Pass Filters (LPF)	No	No	No	No	Yes	No	No	Yes
IF Amplifiers	No	Yes	No	Yes	No	Yes	Yes	Yes
Analog-to-Digital converter (ADC)	No	No	No	Yes	No	No	No	No
Micro-resonator	No	Yes	No	No	No	Yes	Yes	Yes
Duplexer/Switches	Yes	–	Yes	No	No	Yes	–	Yes

summarises the level of integration of the CMOS chips reported in this review.

3.1.4. Microcoil fabrication

Miniaturised microcoil increases the mass sensitivity of NMR measurements [31]. As compared to the signal in larger coils, the induced voltage per mass unit of the sample in microcoil increases as a result of the higher magnetic field sensitivity. A comprehensive introduction to the fundamental physics and characteristics of coils in NMR applications can be found in [32]. Fabricating high quality microcoil remains a challenge to date, despite the latest advances in micro-fabrication technologies [33]. The quality factor of a coil, Q, is an important figure of merit since it corresponds to the ratio of the energy stored to those dissipated. It is defined as $Q = \frac{\omega L}{R}$, with ω the resonant frequency of the resonator, L the coil inductance and R the coil resistance at the resonant frequency [32]. Table 2 lists a large variety of microcoil geometries and fabrication techniques reported to date.

Planar microcoils can be fabricated using standard microfabrication techniques. Typically, photolithography is used to define the pattern of the leads, and a thin layer of seed metal is deposited and copper or gold is electroplated [6,34,35]. The microcoil fabrication process can readily be adapted with CMOS integrated circuit technology to obtain on-chip planar coils [27,29]. On-chip planar coils are typically very lossy due to the thin metal layer (at the order of micrometers), and feature low quality factors. The importance of minimising the contact resistance in order to increase the quality factor and the shortcoming of various coil fabrication techniques was stressed in [36]. A highly original fabrication technique using liquid metal technology which does not require access to a cleanroom was proposed. Gallium, with a low melting temperature of 29.8 °C, is cast into the microfluidic spiral channel. Another approach based on stacked layers fabricated with thin-film technology was reported in [37].

Non-standard coil geometries have been reported in the literature. Microslot geometry has been used to detect the molecular structure in ultra-small samples [38]. A microstrip is a dual-layer structure transporting quasi-transverse RF electromagnetic modes. A microscopic slot produces a pure series inductance. High field strength and quality factors can be achieved, but the field is highly inhomogeneous. The butterfly coil geometry has been considered in [39] to optimise the inner space utilisation of the compact borehole magnet employed in the study. Micro-Helmholtz coils are suitable to facilitate high-resolution μNMR experiments and simplify the interfacing of the sample chamber thanks to this minimally invasive geometry [40].

Fabricating 3D structures (e.g., solenoid or saddle coils) brings a higher level of complexity. Micro solenoid can be obtained with an automatic wire bonding process [41,42] and conveniently wrapped around micro-capillary tubes or an internal structure (typically obtained with photolithography techniques). In [41], a two-solvent method has been introduced to obtain an external support structure of the solenoids, thereby improving the achievable filling factor (i.e., the fraction of the coil volume available for the sample). Solenoid can also be fabricated with 3D photolithography and electroplating techniques can also be used in the fabrication of the solenoid [43] or saddle coils [44]. The cylindrical symmetry of solenoids has been used to develop specific processes. In [45], the solenoid shape is lithographed on the photoresist coating of a metal wire that is simultaneously rotated and translated resulting in the helical translation of the photolithographic mask pattern. [46] used a focused ion beam milling technique to produce a solenoid from a gold/chromium coated layer applied on a tube.

3.2. Compact permanent magnet

Compact permanent magnet has a small footprint and does not require power to generate the magnetic field, which explains their adequacy for portable μNMR applications. The achievable magnetic field strengths with permanent magnets are limited to ~2 T. The neodymium iron boron alloy (NdFeB) is the most widely employed material due to its high remanence and coercivity properties. Its low Curie temperature (150 °C) is still adequate for common μNMR applications. For measurements at high temperature, other materials such as samarium-cobalt can be considered. Inevitably, in low-field NMR experiments, the resonance frequency is low, and so is the magnitude of the NMR signal which scales with B_0^2.

In low-field NMR applications with small permanent magnets, the drift of the B_0-field with the temperature change can be problematic, in particular for experiments with multiple pulse sequences [30]. The temperature coefficient of B_0 for the NdFeB magnet is of the order of −1200 ppm/K. Besides the integration of a temperature controller, which is bulky in size and unbefitting for portable applications, two different approaches to temperature-drift correction have been considered in the design of μNMR systems. [21] adjusts automatically the RF excitation frequency in a feedback loop to match the measured f_L. By sweeping the frequency of the excitation signal and tracking the resulting frequency of the NMR signal, the temperature variation of the magnet can be compensated. Another method proposed by [19] is to stabilise the $\overrightarrow{B_0}$-field with a correction magnetic field induced by a shim coil. The authors employed a Hall-effect magnetic sensor implemented in CMOS technology to sense the static magnetic field from the permanent magnet, elucidating the advantage of the CMOS IC for cooperating different modules on a single chip. The output from the Hall sensor was used to implement a feedback loop to drive the shim coil. The possibility to use a crystal oscillator without frequency synthesizer, benefitting from the stabilised B_0, was highlighted as a major advantage of this approach.

Table 2
Geometries of microcoil and its´ fabrication techniques.

Reference	Coil geometry	Windings	Dimension [μm]	Fabrication process	Material	Frequency [MHz]	Quality factor	Inductance L [nH]
Massin, et al. [35]	Spiral	3	ø: 880	Photolithography & electroplating	Copper	300	23.5	8.7
Lee [6]	Spiral	20	ø: 2500	Photolithography & electroplating	Copper	21.3	16	500
Kong [36]	Spiral	5	ø: 4000	Liquid metal molding	Gallium	21.65	30.4	67.5
Grisi [27]	Spiral	22	ø: 160	CMOS 130 nm technology	Copper	300	1.7	54
Sun [29]	Square	25	W: 2500, L: 2500	CMOS 180 nm technology	–	20.9	1.9	430
Watzlaw,[37]	Square	4 × 5	W: 4000, L: 4000	Thin-film technology & Microstructuring techniques	Gold	17.1	24.3	2140
Lei [39]	Butterfly	7	–	PCB technology	Copper	20	30	354.8
Maguire [38]	Microslot	–	W: 300, L: ~4000	Excimer laser micromachining	Copper	500	256	–
Spengler [40]	Helmotz	2	ø: 1325, H: 600	Photolithography (2D, dry film) & Automatic wire bonding	Copper	500	106	27
Hsieh et al. [44]	Saddle	2	ø: 500, H: 1000	Photolithography & electroplating (3D)	Copper	200	15	–
Sillerud et al. [46]	Solenoid	28	ø: 500, H: 2100	Focused ion beam milling	Gold/Chromium	44.2	10	93
Demas et al. [43]	Solenoid	10	ø: 450, H: 425	Laser Lithography (3D)	Copper	82.7	19	38
Kratt et al. [42]	Solenoid	22	ø: 125 → 1025, H: 550	Photolithography & Automatic wire bonding	Gold	400	52	–
Kamberger et al. [41]	Solenoid	~10	ø: 1500, H: 400/700	Wire bonding & 2-solvent process	Gold	400	44	–

Another limitation of compact permanent magnets is the low achievable $\overrightarrow{B_0}$-field homogeneity, degrading the spectral resolution of μNMR systems and hampering spectroscopy experiments. A few works with compact permanent magnets capable of spectral resolution for low-weight molecules have been reported. Shimming techniques correct the magnetic field inhomogeneities within the sensing volume based on the spherical harmonic decomposition of magnetic resonance calibration images. [30] reports a 0.13 ppm resolution within 1 mm scale with a 0.51 T NdFeB magnet (weighting 7.3 kg) and electrical shimming coils correction. The mechanical shimming technique improving the $\overrightarrow{B_0}$-field homogeneity was introduced in [47]. The method applied to a single-sided magnet and a relatively large sensitive volume (12.5 μL) reported a spectral resolution of 0.25 ppm with a $\overrightarrow{B_0}$-field strength of 0.2 T. [48] shows a mechanical shimming of a 0.7 T compact Halbach-design magnet (weighting 500 g) to yield 0.15 ppm spectral resolution within large samples (5 mm diameter tubes). Still, these milestone achievements do not meet the spectral resolution requirements for studies of large and complex biomolecules.

3.3. Microfluidic technology

Interfacing of the microfluidic technology with μNMR systems is key in many practical PoC medical applications. A review of the advances in microfluidics for diagnosis of infectious diseases can be found in [49]. Microfluidic systems typically serve two basic functions: delivering small amounts of the sample(s) into the sensitive zone of the microcoil and pre-processing of the biological samples.

Fig. 1 illustrates the microfluidic network developed in [6] to mix magnetic nanoparticles (acting as labels) into biological liquid samples, achieving effective mixing upstream with the sample conveyed into the sensitive volume of eight microcoils for multiplexed measurements. [50,51] implements a micro-reaction technology upstream of the NMR measurement for kinetic investigation of reactions with short time constants of only few seconds. Digital microfluidics consists in the manipulation of micro-droplets based on the principle of electro wetting-on-dielectric phenomenon. Electrodes surrounding the microfluidic channels serve a two-fold function of detecting and moving the droplets. [39] described an advanced digital microfluidic system for precise sample delivery.

Biomarker enrichment of the samples can also be achieved with microfluidic technology, based on physical or biological properties. Circulating tumour cells enrichment is key to diagnosing cancer from liquid biopsy samples [52]. Microfluidic cell enrichment of malaria infected red blood cells has been combined with NMR relaxometry detection in [53]. Besides the advantage of increasing the sensitivity of the diagnosis, enrichment has been shown to solve the issue caused by baseline fluctuations between individuals of the relaxation time constants of uninfected blood samples.

4. NMR-based point of care medical applications

Tapping on the miniaturisation of μNMR systems, a number of point-of-care medical applications have been demonstrated recently. These are *in vitro* diagnostic related applications which are largely divided between (immuno-specific) labelling-based or label-free method (Table 3). The μNMR systems highlighted the importance of portability in medical applications and the increased mass sensitivity where liquid biopsy (minimally invasive procedure) is made possible.

4.1. Label-based methods

Magnetic-labelling-based μNMR quantifies the level of biomarker based on variations in relaxation time constants through binding of antigen-targeted magnetic nanoparticles (MNPs), in analogy to the enzyme-linked immunosorbent assay (ELISA). MNP-labelled targets

Table 3
Label-based and label-free medical applications of μNMR reported in this review.

Reference	Label-based/Label-free	Disease	Target biomarker	Biofluid biopsies
Lee [6]	Label-based	Bacteria detection (*S. aureus*); Cancer (breast)	Enzyme (D-alanyl-D-alanine); Protein (HER2 + EGFR)	Sputum, Serum
Haun [59]	Label-based	Cancers (breast, colon, etc.)	Protein (EpCAM + HER2 + EGFR + Mucin1 + CD45)	Blood (CTC)
Haun [60]	Label-based	Cancer (intra-abdominal)	Protein (MUC-1 + HER2 + EGFR + EpCAM)	Tissue
Liong [63]	Label-based	Bacteria detection (M. tubercolosis)	DNA	Sputum
Chung [54]	Label-based	Bacteria detection (S. aureus, *E. faecalis*, *E. coli*, …)	DNA	Tissue
Ghazani [61]	Label-based	Cancer (epithelial)	Protein (EpCAM + EGFR + HER-2 + vimentin)	Blood (CTC)
Neely [65]	Label-based	Sepsis (Candida)	DNA	Whole blood
Snyder [64]	Label-based	Lyme disease	DNA	Whole blood
Gee [62]	Label-based	Cancer (Melanoma)	DNA	Whole blood (CTC)
Lei [14]	Label-based	Immuno-diagnosis; Bacteria detection (E. faecalis)	Protein (Immunoglobulin G) DNA	N/A
Kong [36]	Label-free	Anaemia	Blood oxygenation level, Haematocrit level	Whole blood
Peng [7]	Label-free	Met-haemoglobin	Blood oxidation level	Whole blood
Peng [72] Kong [53]	Label-free	Malaria disease	Hemozoin concentration	Whole blood
Robinson [75]	Label-free	Diabetes mellitus	Composite T_2-relaxation	Serum/plasma
Peng [79]	Label-free	Diabetes mellitus	Oxidative stress in Hb and serum	Whole blood
Cuker [91]	Label-free	Platelet disorder	Platelet	Whole blood

cause much higher transverse relaxation rates due to the local magnetic field perturbation as a consequence of the MNPs clustering. The contrast of relaxation rate (i.e., R_2) which was strongly amplified by the magnetic labelling allows (hyper)sensitive detection down to a single cell level [54,55].

Weissleder and his team in Massachusetts General Hospital are leading the research in this direction [6,54,56]. A wide range of marker targets had been considered in various studies which include the nucleic acids, proteins, target-drug binding, bacteria and tumour cells. The team focuses on using the immuno-specific MNPs with diameters in the range of tens of nanometres [57–59]. These nanoparticles are typically superparamagnetic and are much smaller than the larger beads used for immuno-separation which are ferromagnetic. Since the signal detection is based on the magnetic particles, direct detection on the cells/tissues (without sample purification) is possible. Therefore, the cell loss event is negligible and simplifies assay procedures drastically. Haun et al. then have shown an improved version of the universal labelling approach known as the Biorthogonal Nanoparticle Detection (BOND) [59]. The role of microfluidics in achieving effective mixing of MNPs and target analytes was discussed in [6,58].

Haun et al. reported the detection of tumour cells obtained using fine-needle aspirates in clinical setting [60]. They demonstrated that by using four-protein signature, 96% accuracy for cancer diagnosis was achieved, surpassing the gold-standard immunochemistry. Ghazani et al. compared the diagnosis outcome with bulk tumour and circulating tumour cells (CTC) in peripheral blood samples using μNMR system [61]. Only a weak correlation was found between each paired sample, and thus suggesting that the hype of using of CTC as "liquid biopsies" and proxies to metastatic solid lesions could be misleading. In another separate study on melanoma tumour samples, Gee et al. found a correlation between of melanoma CTC in peripheral blood and a reference tumour evaluation method (RECIST) using μNMR system [62].

Chung et al. presented a magneto-DNA probe using the nanoparticle hybridization assay to detect the amplified target DNAs using micro NMR. It was shown that they were able to detect a panel of 13 bacterial species in hours [54]. Liong et al. used the same platform to detect *Mycobacterium tuberculosis* and identify the drug resistance strain from sputum samples in 2.5 h [63]. Lei et al. recently reported the use of MNP with protein biomarker detection of Immunoglobulin G and with DNA biomarker detection of the *E. faecalis* bacteria [19]. Encouraging clinical tests in detecting sepsis, the severe inflammatory response to infection caused by fungi species Candida, have been reported by the US company T2 Biosystems [65]. Recently, the company also demonstrated the direct detection in whole blood of three species of the *Borrelia* genus responsible for Lyme disease with high sensitivity [64]. Unlike the standard PCR method, target DNA is amplified directly from the whole blood without the use of DNA extraction and purification.

4.2. Label-free methods

Blood contains an abundance of water molecules both intra-cellular (red blood cells, white blood cells, platelets), and extra-cellular (plasma and serum). The read-out of the relaxation rate of the water-molecules in blood is, therefore straightforward and profiling of T_2 relaxation provides vital information reflecting the health status. Haemoglobin (Hb), the iron-containing protein is the major component of red blood cells (RBCs), which accounts for approximately two-thirds of the total blood protein concentration [66]. The heme-iron can exists in various oxidation states depending on the oxidation and oxygenation level of the haemoglobin [67,68]. The *in vitro* μNMR diagnostic is entirely in analogy to blood oxygen level dependant imaging (BOLD) technique [69]. The alteration between oxygenated Hb (HbO_2) and deoxygenated Hb (deoxy-Hb) levels, which is in diamagnetic and paramagnetic state, respectively, reflects the oxygen-uptake of the brain.

Methaemoglobin (met-Hb) is the main oxidation product of Fe(II) to Fe(III) conversion in haemoglobin. Unusually high level of blood oxidation may pose clinical pathological condition known as methemoglobinemia [70]. Methemoglobinemia, which can be either congenital or acquired, is a condition with elevation of met-Hb in the blood. Therefore, there is a clinical need for rapid and accurate determination of met-Hb at point-of-care monitoring. By exploiting the substantial reduction in T_1 and T_2 relaxation time in met-Hb (due to the presence of five unpaired electrons), *in vitro* rapid detection of blood oxidation/oxygenation level using μNMR systems were reported in [36,7], respectively.

Interestingly, hemozoin, which is the metabolic by-product of *Plasmodium* parasites during malaria infection, was used as a natural target of μNMR detection (Fig. 2) [72,73]. The relatively large paramagnetic crystallites [74] created a unique and sensitive read-out against the baseline reading (e.g., healthy and uninfected blood). As a result, the μNMR was able to provide a substantially high level of sensitivity as shown in their mice studies. High level of sensitivity may be used to single out asymptomatic patients or to conduct large randomised screening in the field setting. The research group further demonstrated that low-cost, and higher sensitivity of detection was viable by using microfluidic separation techniques [53]. They demonstrated that by exploiting on the much lower deformability properties of infected RBCs as compared to uninfected normal blood, substantial enrichment was achieved. This method is effective in overcoming the challenges posed by fluctuating baseline readings between individuals.

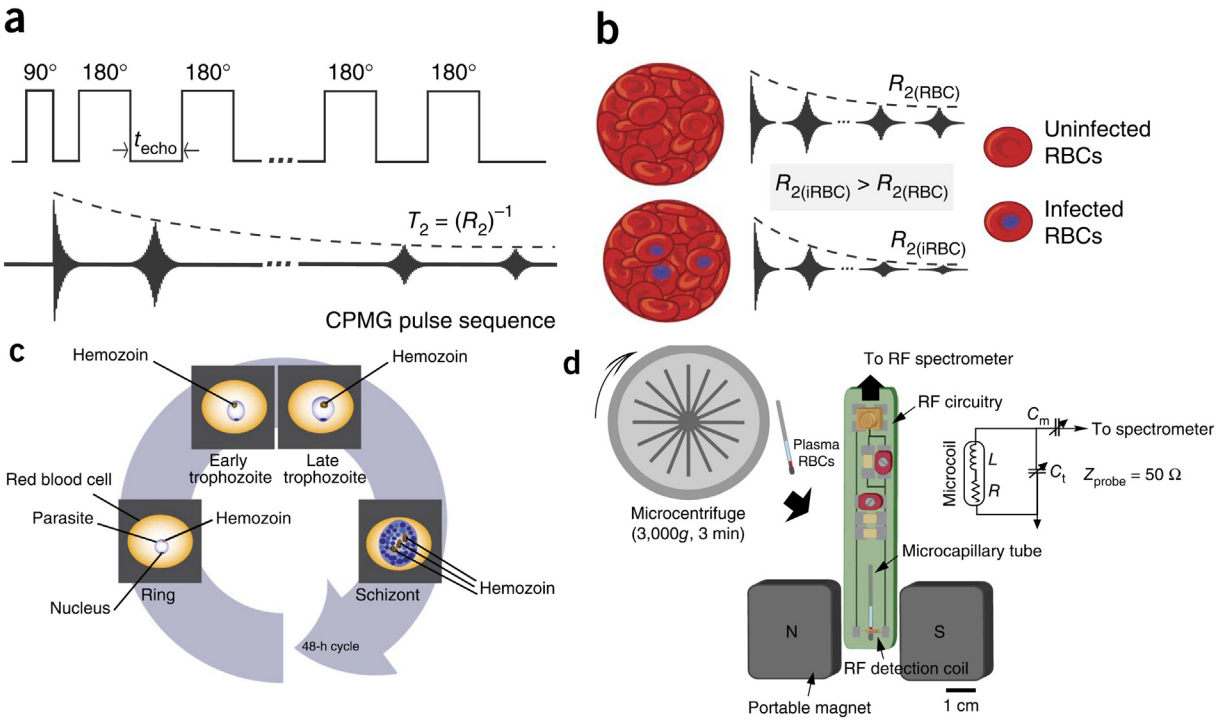

Fig. 2. Micromagnetic resonance relaxometry for rapid and label-free detection in malaria infection. (a) Radio frequency pulse sequence used in the work. (b) The transverse relaxation rate is a function of the parasite load which present in the sample. (c) The 48 h life-cycle of *Plasmodium* parasites and the corresponding parasite/hemozoin load. (d) The benchtop sizedNMR electronic developed in this work. This figure is adapted from [72] and reproduced with permission from Springer Nature.

Cucker et al. [91] developed a rapid assay of platelet function by measuring platelet-mediated clot contraction in small volumes of whole blood using T_2 index by the benchtop NMR. Qualitative platelet disorders (QPDs) comprise a heterogeneous group of conditions characterised by diverse defects in platelet function and a variable tendency to bleed. The current gold-standard for QPDs is the light transmission aggregometry (LTA), which is labour intensive, requires technical expertise, and the methods are not well standardised. They demonstrated that the normal ranges for platelet mediated clot contraction can be established and used these ranges to correlate with patients of known platelet dysfunction. In the 21 healthy donors, the results showed 100% agreement with LTA, while subjects with abnormalities in seven of the patients with known QPDs were detected. This technology has potential to replace the existing clinical diagnosis of QPDs based on LTA, which requires a significantly larger volume of blood, intensive labour, and expertise.

Cistola and his team characterised the hydrocarbon chain structure of fatty acids using benchtop NMR technology [75]. Using multi-exponential decomposition technique, it was shown that T_2 read-out is sensitive to variations in hydrocarbon packing. Hydrocarbon is an interesting subject as the functional properties of lipid-rich assemblies (e.g., serum lipoproteins and cell membranes) are often modulated by the fluidity of the hydrocarbon chain environment. Recently, the team demonstrated the clinical utility of this technique in metabolic syndrome [66,77].

Diabetes mellitus is defined by the persistent elevation of plasma glucose concentration, and metabolic syndrome is often used to identify individuals at risk for type 2 diabetes (T2D). Metabolic syndrome is one of the most prevalent public health problems world-wide. Metabolic syndrome, however is a cluster of clinical findings which includes the combination of insulin resistance, glucose intolerance, abdominal obesity, elevated blood pressure and/or pro-inflammatory state. Cistola and his team proposed using a single measurement of water T_2 in serum/plasma as an early and global marker for metabolic syndrome [78]. In a cross sectional study performed on 72 non-diabetic human subjects, it was shown that the water T_2 in serum/plasma exhibited strong bivariate correlations with markers of insulin, lipids, inflammation, coagulation, and electrolyte balance.

Recently, the team employed modified DNA aptamers to determine the relative concentrations of 1310 proteins [77]. They found five new proteins which are the most predictive of water T_2: hepatocyte growth factor, receptor tyrosine kinase FLT3, bone sialoprotein 2, glucokinase regulatory protein and endothelial cell-specific molecule. Hepatocyte growth factor has been associated with high rates of T2D incidents, while the endothelial cell specific molecule is associated with atherosclerosis in subjects with diabetes. Glucokinase regulatory protein plays an important role in hepatic glucose uptake and is used as drug target for T2D.

In parallel to this development, Peng and his team recently proposed that functional phenotyping of oxidative stress in the blood enables read-out of individual's oxidative status, susceptibility and capacity. This yields significantly richer and clinically useful information as compared to routine biomarkers. The group demonstrated that using μNMR system, oxidative stress can be used as additional marker to substratify diabetes mellitus patients, in association to the subjects´ glycemic profile [79].

The presence of natural biomarkers (e.g., oxygenation/oxidation, oxidative stress, hemozoin), alter the baseline reading of the blood (T_2-contrast), making the label-free μNMR technique a strong candidate for clinical disease care and management (e.g., diagnosis, prognosis, and monitoring) at point-of-use. Liquid biopsies of blood sample (as opposed to tissue biopsies) are minimally invasive and provide a snapshot of the health status. In addition, blood samples can be easily processed using the standard benchtop centrifuge and micro capillary tubes/haematocrit tubes can be adapted into the μNMR system for one-stop measurements.

5. Conclusion and future outlook

Recent technological progress in micro- and nanofabrication technologies relevant to the development of μNMR systems motivates many new medical applications for point-of-care diagnosis or limited sample analysis. Progress in CMOS technology enables low-cost and large-scale integration of transistors and physical sensing materials on a single chip, combining seamlessly the two key enabling functions of bio-sensing devices: signal transducing and signal processing. Apart from lowering of engineering barriers (e.g., low-power, low-cost and much higher portability), the non-invasiveness property of NMR [18], which allows *ex vivo* (direct) characterization of liquid/tissues biopsies has opened up new avenues in the interest of personalised medicine (e.g., functional assays [79]). Functional assay has large implication as it allows assessments of cells/tissues activity qualitatively and quantitatively, in a manner which is time- and patient-unique. This may be useful for disease prognosis (or monitoring) for chronic disease, where the complication(s) may develop as the consequence of the disease. On the other spectrum, *in vivo* application such as NMR-based (or MRI-based) wearable device or compact body fluids analyser for monitoring may become feasible in near future [2,80].

With the recent development of the fast and highly efficient multi-dimensional inverse Laplace decomposition algorithm [81–83], two- and multi-dimensional NMR relaxometry applications in the low-field are highly feasible [84,85]. Combined with the implementation of ultrafast acquisition techniques as shown by Ahola and coworkers [84,87] practical and useful real-time medical application may soon be possible. Scaling up to higher dimensions (e.g., two or multi-dimensional) spectroscopy provides much more information which corresponds to building a ´virtual´ panel of biomarkers in a single scan. With the increased information (or markers), the diagnostic prediction would be much higher, and disease sub-stratification would be possible. Interestingly, the physics of NMR enables the flexibility of creating NMR-based biomarkers unique to the biological system, and independent of existing -omics. Among others, information on water-protein interaction [86] and protein-protein interaction [87] may help to extend the markers library. Encoding the biochemical and biophysical information (e.g., molecular rotational, diffusional motion) into the relaxation times frame, namely the T_1 and T_2, it can show molecular information even from the portable low field μNMR systems. Interestingly, the relaxation properties can be used as a highly sensitive and specific molecular probe, and provide important molecular motion (e.g., correlational relaxation, diffusion properties), which is not readily available in NMR spectra in the frequency domain.

On the other hand, with the improved spectral resolution using small footprint permanent magnets [30], the application of low-field NMR spectroscopy (in frequency domain) at point-of-use setting is accelerated. In the field of metabolomics, NMR spectroscopy in combination with multivariate statistical analysis and pattern recognition methods showed potential in profiling the metabolic status of organisms and diagnosing diseases [88]–[90]. Further advances in magnet shimming technologies may in the future enable NMR spectroscopy using compact μNMR systems for metabolomics at point-of-care settings.

Conflict of interest

None.

Acknowledgements

W.K. Peng would like to acknowledge the support of INL Start Up Grant.

References

[1] B. Blümich, K. Singh, Desktop NMR and its applications from materials science to organic chemistry, Angew. Chem. Int. Ed. 57 (24) (Jun, 2018) 6996–7010.
[2] B. Blümich, Beyond compact NMR, Microporous Mesoporous Mater. 269 (Oct, 2018) 3–6.
[3] J. van Duynhoven, A. Voda, M. Witek, H. van As, Annual Reports on NMR Spectroscopy, 69 (2010) 145–197.
[4] N. Ravi, G. Rizzi, S.E. Chang, P. Cheung, P.J. Utz, S.X. Wang, Quantification of cDNA on GMR biosensor array towards point-of-care gene expression analysis, Biosens. Bioelectron. 130 (April, 2019) 338–343, https://doi.org/10.1016/j.bios.2018.09.050.
[5] N. Guo, K.W. Cheung, H. Wong, D. Ho, CMOS time-resolved, contact, and multi-spectral fluorescence imaging for DNA molecular diagnostics, Sensors 14 (11) (Oct, 2014) 20602–20619.
[6] H. Lee, E. Sun, D. Ham, R. Weissleder, Chip–NMR biosensor for detection and molecular analysis of cells, Nat. Med. 14 (8) (Aug, 2008) 869–874.
[7] W.K. Peng, L. Chen, J. Han, Development of miniaturized, portable magnetic resonance relaxometry system for point-of-care medical diagnosis, Rev. Sci. Instrum. 83 (9) (2012) 095115, https://doi.org/10.1063/1.4754296.
[8] J. Handwerker, B. Schlecker, M. Ortmanns, J. Anders, Integrated circuit technology for next generation point-of-care spectroscopy applications, IEEE Commun. Mag. 55 (10) (Oct, 2017) 143–151.
[9] K.-M. Lei, P.-I. Mak, M.-K. Law, R.P. Martins, CMOS biosensors for in vitro diagnosis – transducing mechanisms and applications, Lab Chip 16 (19) (2016) 3664–3681.
[10] K. Lee, S. Choi, J.O. Lee, J. Yoon, G. Cho, CMOS capacitive biosensor with enhanced sensitivity for label-free DNA detection, 2012 IEEE International Solid-State Circuits Conference, 2012, pp. 120–122.
[11] A. Manickam, A. Chevalier, M. McDermott, A.D. Ellington, A. Hassibi, A CMOS electrochemical impedance spectroscopy (EIS) biosensor array, IEEE Trans. Biomed. Circ. Syst. 4 (6) (Dec, 2010) 379–390.
[12] J. Anders, Micro and Nano Scale NMR: Technologies and Systems, Wiley-VCH, Weinheim, 2018.
[13] B. Blümich, Introduction to compact NMR: a review of methods, TrAC Trends Anal. Chem. 83 (Oct, 2016) 2–11.
[14] K.-M. Lei, P.-I. Mak, M.-K. Law, R.P. Martins, Handheld Total Chemical and Biological Analysis Systems: Bridging NMR, Digital Microfluidics, and Semiconductors, Springer, 2017.
[15] K.-M. Lei, N. Sun, P.-I. Mak, R.P. Martins, D. Ham, Micro-NMR on CMOS for biomolecular sensing, CMOS Circuits for Biological Sensing and Processing, Springer, Cham, 2018, pp. 101–132.
[16] M.H. Levitt, Spin Dynamics: Basics of Nuclear Magnetic Resonance, 2nd ed., John Wiley & Sons, Chichester, England; Hoboken, NJ, 2008.
[17] W.G. Proctor, F.C. Yu, The dependence of a nuclear magnetic resonance frequency upon chemical compound, Phys. Rev. B 77 (Mar, 1950).
[18] F. Bloch, Nuclear induction, Phys. Rev. 70 (7–8) (Oct, 1946) 460–474.
[19] K.M. Lei, H. Heidari, P.I. Mak, M.K. Law, F. Maloberti, R.P. Martins, A handheld high-sensitivity micro-NMR CMOS platform with B-field stabilization for multi-type biological #x002F;chemical assays, IEEE J. Solid State Circuits 52 (1) (2017) 284–297.
[20] J. Kim, B. Hammer, R. Harjani, A 5-300MHz CMOS Transceiver for Multi-Nuclear NMR Spectroscopy, (2012), pp. 1–4.
[21] D. Issadore, C. Min, M. Liong, J. Chung, R. Weissleder, H. Lee, Miniature magnetic resonance system for point-of-care diagnostics, Lab Chip 11 (13) (2011) 2282.
[22] K. Takeda, OPENCORE NMR: open-source core modules for implementing an integrated FPGA-based NMR spectrometer, J. Magn. Reson. 192 (2) (Jun, 2008) 218–229.
[23] N.N. Vo, L. Chen, X. Liu, W.K. Peng, Z.Y. Ming, J. Han, Highly integrated, low cost, palm-top sized magnetic resonance relaxometry system for rapid blood screening, in: J. Goh (Ed.), The 15th International Conference on Biomedical Engineering, vol. 43, Springer International Publishing, Cham, 2014, pp. 558–561.
[24] N. Sun, Y. Liu, H. Lee, R. Weissleder, D. Ham, CMOS RF biosensor utilizing nuclear magnetic resonance, IEEE J. Solid State Circuits 44 (5) (May, 2009) 1629–1643.
[25] J. Anders, P. SanGiorgio, G. Boero, An Integrated CMOS Receiver Chip for NMR-Applications, (2009), pp. 471–474.
[26] J. Anders, J. Handwerker, M. Ortmanns, G. Boero, A low-power high-sensitivity single-chip receiver for NMR microscopy, J. Magn. Reson. 266 (May, 2016) 41–50.
[27] M. Grisi, G. Gualco, G. Boero, A broadband single-chip transceiver for multi-nuclear NMR probes, Rev. Sci. Instrum. 86 (4) (Apr, 2015) 044703.
[28] Y. Liu, N. Sun, H. Lee, R. Weissleder, D. Ham, CMOS Mini Nuclear Magnetic Resonance System and its Application for Biomolecular Sensing, (2008), pp. 140–602.
[29] N. Sun, T.J. Yoon, H. Lee, W. Andress, R. Weissleder, D. Ham, Palm NMR and 1-Chip NMR, IEEE J. Solid State Circuits 46 (1) (Jan, 2011) 342–352.
[30] D. Ha, J. Paulsen, N. Sun, Y.-Q. Song, D. Ham, Scalable NMR spectroscopy with semiconductor chips, Proc. Natl. Acad. Sci. 111 (33) (Aug, 2014) 11955–11960.
[31] D.L. Olson, T.L. Peck, A.G. Webb, R.L. Magin, J.V. Sweedler, High-resolution microcoil 1H-NMR for mass-limited, nanoliter-volume samples, Science 270 (5244) (Dec, 1995) 1967–1970.
[32] A. Haase, et al., NMR probeheads forin vivo applications, Concepts Magn. Reson. 12 (6) (2000) 361–388.
[33] A.G. Webb, Radiofrequency microcoils for magnetic resonance imaging and spectroscopy, J. Magn. Reson. 229 (Apr, 2013) 55–66.
[34] J. Dechow, A. Forchel, T. Lanz, A. Haase, Fabrication of NMR — microsensors for nanoliter sample volumes, Microelectron. Eng. 53 (1) (Jun, 2000) 517–519.

[35] C. Massin, G. Boero, F. Vincent, J. Abenhaim, P.-A. Besse, R.S. Popovic, High-Q factor RF planar microcoils for micro-scale NMR spectroscopy, Sensors Actuators A Phys. 97–98 (Apr, 2002) 280–288.
[36] T.F. Kong, W.K. Peng, T.D. Luong, N.-T. Nguyen, J. Han, Adhesive-based liquid metal radio-frequency microcoil for magnetic resonance relaxometry measurement, Lab Chip 12 (2) (2012) 287–294.
[37] J. Watzlaw, S. Glöggler, B. Blümich, W. Mokwa, U. Schnakenberg, Stacked planar micro coils for single-sided NMR applications, J. Magn. Reson. 230 (May, 2013) 176–185.
[38] Y. Maguire, I.L. Chuang, S. Zhang, N. Gershenfeld, Ultra-small-sample molecular structure detection using microslot waveguide nuclear spin resonance, Proc. Natl. Acad. Sci. 104 (22) (May, 2007) 9198–9203.
[39] K.-M. Lei, P.-I. Mak, M.-K. Law, R.P. Martins, A palm-size μNMR relaxometer using a digital microfluidic device and a semiconductor transceiver for chemical/biological diagnosis, Analyst 140 (15) (2015) 5129–5137.
[40] N. Spengler, et al., Heteronuclear micro-Helmholtz coil facilitates μm-range spatial and sub-Hz spectral resolution NMR of nL-volume samples on customisable microfluidic chips, PLoS One 11 (1) (Jan, 2016) e0146384.
[41] R. Kamberger, A. Moazenzadeh, J.G. Korvink, O.G. Gruschke, Hollow microcoils made possible with external support structures manufactured with a two-solvent process, J. Micromech. Microeng. 26 (6) (2016) 065002.
[42] K. Kratt, V. Badilita, T. Burger, J.G. Korvink, U. Wallrabe, A fully MEMS-compatible process for 3D high aspect ratio micro coils obtained with an automatic wire bonder, J. Micromech. Microeng. 20 (1) (Jan, 2010) 015021.
[43] V. Demas, et al., Electronic characterization of lithographically patterned microcoils for high sensitivity NMR detection, J. Magn. Reson. 200 (1) (Sep, 2009) 56–63.
[44] C.Y. Hsieh, Y.T. Yeh, L.S. Fan, Multilayer high-aspect-ratio RF coil for NMR applications, Microsyst. Technol. 17 (8) (Aug, 2011) 1311–1317.
[45] D. Lee, H. Hiroshima, Y. Zhang, T. Itoh, R. Maeda, Cylindrical projection lithography for microcoil structures, Microelectron. Eng. 88 (8) (Aug, 2011) 2625–2628.
[46] L.O. Sillerud, et al., 1H NMR detection of superparamagnetic nanoparticles at 1T using a microcoil and novel tuning circuit, J. Magn. Reson. 181 (2) (Aug, 2006) 181–190.
[47] J. Perlo, F. Casanova, B. Blümich, Ex situ NMR in highly homogeneous fields: 1H spectroscopy, Science 315 (5815) (Feb, 2007) 1110–1112.
[48] E. Danieli, J. Perlo, B. Blümich, F. Casanova, Small magnets for portable NMR spectrometers, Angew. Chem. Int. Ed. 49 (24) (2010) 4133–4135.
[49] A. Tay, A. Pavesi, S.R. Yazdi, C.T. Lim, M.E. Warkiani, Advances in microfluidics in combating infectious diseases, Biotechnol. Adv. 34 (4) (Jul, 2016) 404–421.
[50] A. Brächer, et al., Thermostatted micro-reactor NMR probe head for monitoring fast reactions, J. Magn. Reson. 242 (May, 2014) 155–161.
[51] A. Brächer, R. Behrens, E. von Harbou, H. Hasse, Application of a new micro-reactor 1H NMR probe head for quantitative analysis of fast esterification reactions, Chem. Eng. J. 306 (Dec, 2016) 413–421.
[52] C. Alix-Panabières, K. Pantel, Challenges in circulating tumour cell research, Nat. Rev. Cancer 14 (9) (2014) 623–631.
[53] T.F. Kong, et al., Enhancing malaria diagnosis through microfluidic cell enrichment and magnetic resonance relaxometry detection, Sci. Rep. 5 (Jun, 2015) 11425.
[54] H.J. Chung, C.M. Castro, H. Im, H. Lee, R. Weissleder, A magneto-DNA nanoparticle system for rapid detection and phenotyping of bacteria, Nat. Nanotechnol. 8 (5) (May, 2013) 369–375.
[55] Z.-X. Luo, L. Fox, M. Cummings, T.J. Lowery, E. Daviso, New frontiers in in vitro medical diagnostics by low field T2 magnetic resonance relaxometry, TrAC Trends Anal. Chem. 83 (Oct, 2016) 94–102.
[56] L. Josephson, J.M. Perez, R. Weissleder, Magnetic nanosensors for the detection of oligonucleotide sequences, Angew. Chem. 113 (17) (Sep, 2001) 3304–3306.
[57] C.M. Castro, et al., Miniaturized nuclear magnetic resonance platform for detection and profiling of circulating tumor cells, Lab Chip 14 (1) (2014) 14–23.
[58] H. Lee, T.-J. Yoon, J.-L. Figueiredo, F.K. Swirski, R. Weissleder, Rapid detection and profiling of cancer cells in fine-needle aspirates, Proc. Natl. Acad. Sci. U. S. A. 106 (30) (Jul, 2009) 12459–12464.
[59] J.B. Haun, N.K. Devaraj, S.A. Hilderbrand, H. Lee, R. Weissleder, Bioorthogonal chemistry amplifies nanoparticle binding and enhances the sensitivity of cell detection, Nat. Nanotechnol. 5 (9) (Sep, 2010) 660–665.
[60] J.B. Haun, et al., Micro-NMR for rapid molecular analysis of human tumor samples, Sci. Transl. Med. 3 (71) (Feb, 2011) 71ra16.
[61] A.A. Ghazani, et al., Comparison of select cancer biomarkers in human circulating and bulk tumor cells using magnetic nanoparticles and a miniaturized micro-NMR system, Nanomedicine 9 (7) (Oct, 2013) 1009–1017.
[62] M.S. Gee, et al., Point of care assessment of melanoma tumor signaling and metastatic burden from μNMR analysis of tumor fine needle aspirates and peripheral blood, Nanomedicine 13 (3) (Apr, 2017) 821–828.
[63] M. Liong, et al., Magnetic barcode assay for genetic detection of pathogens, Nat. Commun. 4 (1) (Dec, 2013).
[64] J.L. Snyder, et al., T2 magnetic resonance-based direct detection of three Lyme disease-related Borrelia species in whole blood samples, J. Clin. Microbiol. (May, 2017) 00510–00517.
[65] L.A. Neely, et al., T2 magnetic resonance enables nanoparticle-mediated rapid detection of candidemia in whole blood, Sci. Transl. Med. 5 (182) (Apr, 2013) 182ra54.
[66] D.P. Cistola, M.D. Robinson, Compact NMR relaxometry of human blood and blood components, TrAC Trends Anal. Chem. 83 (Oct, 2016) 53–64.
[67] M.-E. Meyer, O. Yu, B. Eclancher, D. Grucker, J. Chambron, NMR relaxation rates and blood oxygenation level, Magn. Reson. Med. 34 (2) (Aug, 1995) 234–241.
[68] K.R. Thulborn, J.C. Waterton, P.M. Matthews, G.K. Radda, Oxygenation dependence of the transverse relaxation time of water protons in whole blood at high field, Biochim. Biophys. Acta 714 (2) (Feb, 1982) 265–270.
[69] S. Ogawa, T.M. Lee, A.R. Kay, D.W. Tank, Brain magnetic resonance imaging with contrast dependent on blood oxygenation, Proc. Natl. Acad. Sci. 87 (24) (Dec, 1990) 9868–9872.
[70] S. Aime, M. Fasano, S. Paoletti, A. Arnelli, P. Ascenzi, NMR relaxometric investigation on human methemoglobin and fluoromethemoglobin. An improved quantitativein vitro assay of human methemoglobin, Magn. Reson. Med. 33 (6) (Jun, 1995) 827–831.
[72] W.K. Peng, et al., Micromagnetic resonance relaxometry for rapid label-free malaria diagnosis, Nat. Med. 20 (9) (2014) 1069–1073.
[73] J. Han, W.K. Peng, Reply to 'Considerations regarding the micromagnetic resonance relaxometry technique for rapid label-free malaria diagnosis, Nat. Med. 21 (12) (Dec, 2015) 1387–1389.
[74] L.M. Coronado, C.T. Nadovich, C. Spadafora, Malarial hemozoin: from target to tool, Biochim. Biophys. Acta Gen. Subj. 1840 (6) (Jun, 2014) 2032–2041.
[75] M.D. Robinson, D.P. Cistola, Nanofluidity of fatty acid hydrocarbon chains as monitored by benchtop time-domain nuclear magnetic resonance, Biochemistry 53 (48) (Dec, 2014) 7515–7522.
[77] V. Patel, A.K. Dwivedi, S. Deodhar, I. Mishra, D.P. Cistola, Aptamer-based search for correlates of plasma and serum water T2: implications for early metabolic dysregulation and metabolic syndrome, Biomark. Res. 6 (1) (Dec, 2018).
[78] M.D. Robinson, et al., Water T2 as an early, global and practical biomarker for metabolic syndrome: an observational cross-sectional study, J. Transl. Med. 15 (1) (Dec, 2017).
[79] Peng, W.K., Han, J., and Loh, T.P. (2016). Micro magnetic resonance relaxometry. Patent: WO 2016/172650 A1.
[80] C.Z. Cooley, et al., Two-dimensional imaging in a lightweight portable MRI scanner without gradient coils: lightweight MRI scanner without gradient coils, Magn. Reson. Med. 73 (2) (Feb, 2015) 872–883.
[81] Y.-Q. Song, L. Venkataramanan, M.D. Hürlimann, M. Flaum, P. Frulla, C. Straley, T1–T2 correlation spectra obtained using a fast two-dimensional Laplace inversion, J. Magn. Reson. 154 (2) (Feb, 2002) 261–268.
[82] P. Berman, O. Levi, Y. Parmet, M. Saunders, Z. Wiesman, Laplace inversion of low-resolution NMR Relaxometry data using sparse representation methods, Concepts Magn. Reson. 42 (3) (May, 2013) 72–88.
[83] S. Ahola, et al., Ultrafast multidimensional Laplace NMR for a rapid and sensitive chemical analysis, Nat. Commun. 6 (1) (Dec, 2015).
[84] E. Curti, E. Carini, M.F. Cobo, T. Bocher, E. Vittadini, The use of two-dimensional NMR relaxometry in bread staling: a valuable tool? Food Chem. 237 (Dec, 2017) 766–772.
[85] T. Jeoh, N. Karuna, N.D. Weiss, L.G. Thygesen, Two-dimensional ^{1}H-nuclear magnetic resonance relaxometry for understanding biomass recalcitrance, ACS Sustain. Chem. Eng. 5 (10) (Oct, 2017) 8785–8795.
[86] P.W. Fenimore, H. Frauenfelder, B.H. McMahon, R.D. Young, Bulk-solvent and hydration-shell fluctuations, similar to - and -fluctuations in glasses, control protein motions and functions, Proc. Natl. Acad. Sci. 101 (40) (Oct, 2004) 14408–14413.
[87] N. Nishida, I. Shimada, An NMR method to study protein–protein interactions, in: M. Shimaoka (Ed.), Integrin and Cell Adhesion Molecules, vol. 757, Humana Press, Totowa, NJ, 2011, pp. 129–137.
[88] M.E. Bollard, E.G. Stanley, J.C. Lindon, J.K. Nicholson, E. Holmes, NMR-based metabonomic approaches for evaluating physiological influences on biofluid composition, NMR Biomed. 18 (3) (May, 2005) 143–162.
[90] M.R. Viant, B.G. Lyeth, M.G. Miller, R.F. Berman, An NMR metabolomic investigation of early metabolic disturbances following traumatic brain injury in a mammalian model, NMR Biomed. 18 (8) (Dec, 2005) 507–516.
[91] A. Cuker, et al., Rapid Evaluation of Platelet Function With T2 Magnetic Resonance, Am. J. Clin. Pathol. 146 (6) (Dec, 2016) 681–693.

Further Reading

[89] I.F. Duarte, S.O. Diaz, A.M. Gil, NMR metabolomics of human blood and urine in disease research, J. Pharm. Biomed. Anal. 93 (May, 2014) 17–26.